Available online at www.sciencedirect.com
ScienceDirect
Journal of Sound and Vibration 299 (2007) 12–21
JOURNAL OF SOUND AND VIBRATION
www.elsevier.com/locate/jsvi

Development of adaptive algorithm for active sound quality control

Sen M. Kuo[a], Abhijit Gupta[b,*], Sridevi Mallu[a]

[a]*Department of Electrical Engineering, Center for Acoustics and Vibration, Northern Illinois University, DeKalb, IL 60115, USA*
[b]*Department of Mechanical Engineering, Center for Acoustics and Vibration, Northern Illinois University, DeKalb, IL 60115, USA*

Received 5 July 2005; received in revised form 19 April 2006; accepted 16 June 2006
Available online 28 August 2006

Abstract

This paper develops an active sound-quality control (ASQC) system based on the active noise equalization (ANE) technique, and optimizes it with the filtered-error least mean square (FELMS) algorithm and normalized reference signal generator. The ASQC system controls the sound quality of products such as engines by changing the amplitudes of harmonics. This optimized system uses the FELMS algorithm to limit disturbances in the passband caused by uncorrelated interferences with high gains in the secondary path, thereby increasing the system stability. It achieves fast convergence by normalizing the amplitudes of internally generated sinusoids in the reference signal according to the magnitude response of the secondary path at the corresponding frequencies. Computer simulations demonstrate the desired spectral shaping capability with faster convergence and reduced passband disturbance.

1. Introduction

Active noise control (ANC) [1,2] uses the principle of superposition, whereby a secondary noise of equal amplitude and opposite phase cancels an unwanted primary noise. In many practical ANC applications, the primary noise produced by rotating machines (such as engines) is periodic and contains multiple harmonic-related narrowband components. In the periodic ANC system, a nonacoustic sensor such as a tachometer or an accelerometer [3] can replace the reference microphone. The sensor output synchronizes an internally generated reference signal, thus preventing feedback from the secondary source to the reference sensor. This periodic ANC system was analyzed in Ref. [4] using the filtered-X least mean square (FXLMS) algorithm [5], where the reference signal is filtered by an estimate of the secondary path for updating the adaptive filter's coefficients.

The design of an ANC system usually pursues maximal attenuation of the primary noise. However, in some applications, it is desirable to retain a small residual noise with a specified spectral shape. For example, in an automobile, or earth-moving machine, the driver needs some audible information about engine speed to be able to control the vehicle safely. Active sound-quality control is another potential use of ANC, which changes

*Corresponding author. Tel.: +1 815 753 9379; fax: +1 815 753 0416.
E-mail address: gupta@ceet.niu.edu (A. Gupta).

0022-460X/$ - see front matter
doi:10.1016/j.jsv.2006.06.038

Nomenclature

ASQC	active sound quality control
ANE	active noise equalization
FELMS	filtered-error least mean square
$S(z)$	secondary Path
$\hat{S}(z)$	estimate of secondary path
$W(z)$	output of the adaptive filter
β	gain
$e(n)$	residual noise
$e'(n)$	pseudo error
$x(n)$	input (single-frequency sine wave)
μ	step size
$d(n)$	primary noise
$H(z)$	closed-loop transfer function
$u(n)$	sinusoidal components
$v(n)$	uncorrelated components
$s(n)$	impulse response
*	linear convolution
C	amplitude of reference signal
ϕ	initial phase
ψ	phase shift
A	gain
$C(z)$	adaptive filter
$e_c(n)$	instantaneous squared error signal
$H_c(z)$	transfer function of adaptive comb filter
r	pole radius
S_k	gain of $S(z)$ at frequency ω_k
R	input autocorrelation matrix
λ_{2K}	smallest nonzero eigenvalue of the matrix **R**
$A_k = 1/S_k$	amplitude at ω_k

(amplifies or attenuates with predetermined values) the amplitudes of noise components to improve sound quality or change noise signature. These demands lead to an extension of the ANC concept to include ASQC.

The equalization system for periodic noise with multiple harmonics is called a narrowband ANE, which has been developed in Refs. [6,7]. This algorithm also has been implemented and analyzed in the frequency domain [8], and extended to equalize broadband noise [9]. The fundamental difference between the narrowband ANC and ANE is the system transfer functions. The magnitude response of the narrowband ANC system presents multiple notches with infinite nulls at controlled frequencies, so that the system attenuates those noise components completely. However, the depths of individual notches of the narrowband ANE system are independently adjustable and can even be changed to peaks with predetermined amplitudes without affecting the characteristics of other notches.

Active sound-quality control using the narrowband ANE algorithm inherits the problems of ANC systems with the FXLMS algorithm. These include passband disturbances due to uncorrelated interference at frequencies where the magnitude response of the secondary path has high gain [10], and slow convergence due to the eigenvalue spread of the input autocorrelation matrix determined by the magnitude response of the secondary path [11]. This paper modifies the solutions [10,11] for solving these two critical problems in ANC systems, integrates them with the narrowband ANE [6,7], and presents the optimized ASQC algorithm [12].

2. Narrowband active sound-quality control

A block diagram of the general narrowband ANE system for controlling periodic noise is shown in Fig. 1, where $\hat{S}(z)$ is an estimate of $S(z)$, which is the secondary path from the output of the adaptive filter $W(z)$ to the output of error microphone. The output $y(n)$ of the two-weight filter is split into two branches, the canceling branch and the balancing branch. The gains β and $(1-\beta)$ are inserted in these two branches to adjust the residual noise. Instead of minimizing the residual noise $e(n)$ measured by the error microphone, the ANE system minimizes the computed pseudo error $e'(n)$.

For analysis purpose, we assume a single-frequency sine wave as the input $x(n)$, although this system can be extended to equalize multiple sine waves by connecting several adaptive filters in parallel. For controlling a single-frequency sinusoidal noise, a pure sinewave is internally generated as the reference signal, and the adaptive filter contains two coefficients. This adaptive filter minimizes the instantaneous squared pseudo-error signal using the least mean square (LMS) algorithm [13] expressed as

$$w_i(n+1) = w_i(n) + 2\mu e'(n)x_i(n), \quad i = 1, 2, \tag{1}$$

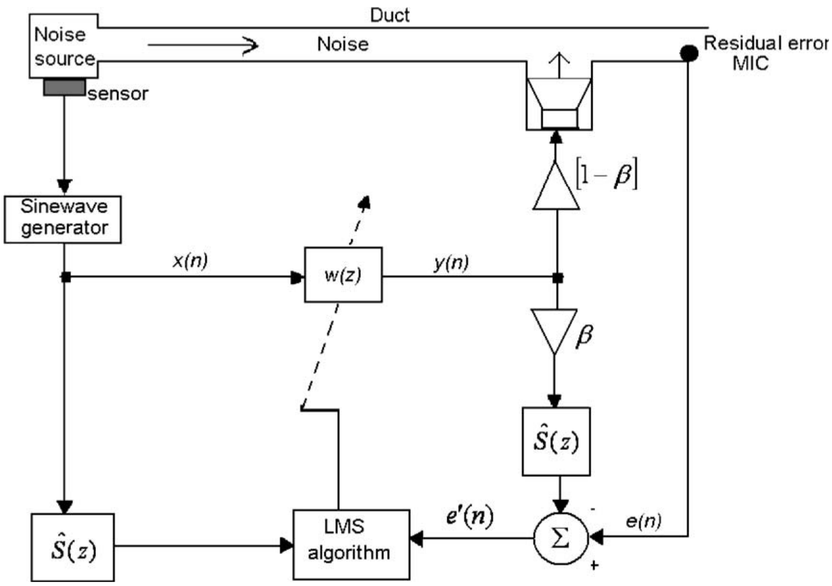

Fig. 1. Block diagram of narrowband ANE system.

where μ is the step size that determines the stability, convergence speed, and steady-state performance of the algorithm.

Fig. 1 shows that if the secondary-path estimate is perfect [i.e., $\hat{S}(z) = S(z)$], the pseudo error $e'(n)$ can be expressed as

$$e'(n) = d(n) - y(n), \tag{2}$$

which is the residual noise of the conventional ANC system, and $d(n)$ is the primary noise generated from the noise source. After the filter has converged, $e'(n) \approx 0$. From Eq. (2), the system output at the reference frequency after convergence is

$$e(n) = d(n) - (1 - \beta)y(n) = \beta\, y(n) \approx \beta\, d(n). \tag{3}$$

This equation shows that the actual system output $e(n)$ contains a narrowband noise whose amplitude can be continuously, linearly, and totally controlled by adjusting the gain value β. The signal $e'(n)$ acts as a pseudo error to "trick" the LMS algorithm so that it will converge to an optimum solution to minimize $e'(n)$, while the actual residual noise $e(n)$ has the desired amplitude as indicated by Eq. (3).

The capability of the ANE system can be determined by evaluating the frequency response of the system at the reference frequency ω_0. Assuming $S(z) = 1$, the closed-loop transfer function $H(z)$ is [6]

$$H(z) = \frac{z^2 - 2z(1 - \beta k)\cos(\omega_0) + (1 - 2\beta k)}{z^2 - 2z(1 - k)\cos(\omega_0) + (1 - 2k)}. \tag{4}$$

Therefore, the poles of system are the same as in an ANC system; however, the zeros are modified as

$$z_z = r_z \exp(\pm j\theta_z), \tag{5}$$

where the radius is

$$r_z = \sqrt{1 - \beta\mu A^2}, \tag{6}$$

and the angle is

$$\theta_z = \cos^{-1}\left[\frac{(1 - \mu\beta A^2/2)\cos\omega_0}{\sqrt{1 - \mu\beta A^2}}\right]. \tag{7}$$

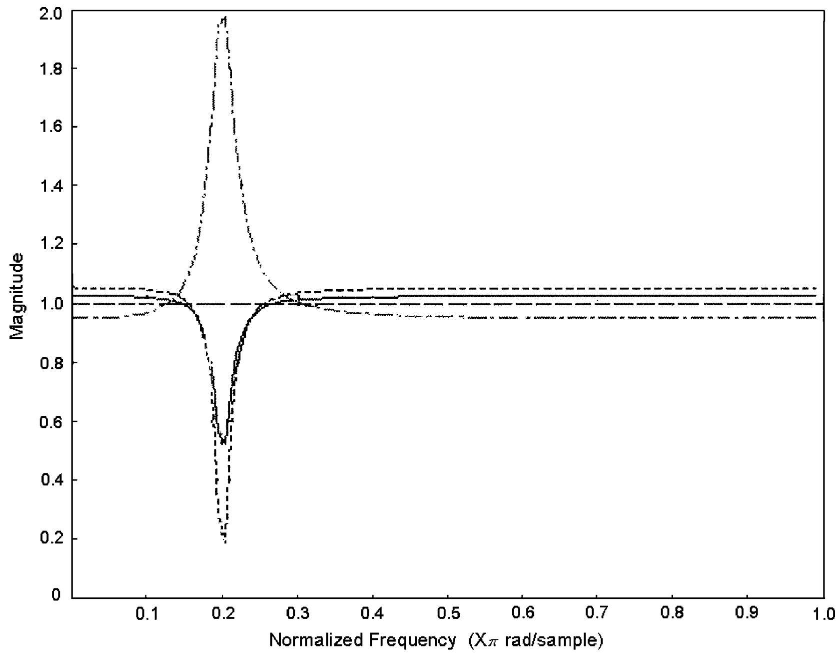

Fig. 2. Amplitude responses of the transfer function for various β values, – – – – $\beta = 0$, ········ $\beta = 0.5$, —— —— $\beta = 1$, – ····· – $\beta = 2$.

The performance of the ANE is determined by the relative position of the poles and zeros of the system. Eq. (6) shows that the zeros are moved by adjusting the value of β. When the zeros of the system move into different regions, the ANE system will perform different functions. These functions can be classified into four modes: (1) Cancellation mode ($\beta = 0$), whereby the zeros are on the unit circle and the ANE attenuates the sinusoid completely at frequency ω_0; (2) Attenuation mode ($0 < \beta < 1$), whereby the zeros lie between the poles and the unit circle and approach the corresponding poles as β increases from 0 to 1, so that the amount of attenuation is determined by the factor β; (3) Neutral mode ($\beta = 1$), whereby the poles are canceled by the zeros and the system has no effect; and (4) Enhancement mode ($\beta > 1$), whereby the zeros are farther away from the unit circle than the poles are and therefore, $H(z)$ exhibits a resonance at frequency ω_0 such that it functions as an amplifier. Examples of the magnitude responses of $H(z)$ for $\beta = 0$, 0.5, 1, and 2 are shown in Fig. 2.

The optimum weight vector of the narrowband ANE is independent of the gain value β. Therefore, the system will converge to the same weight vector regardless of the operating mode of the system. Fig. 3 shows the simulation results of ANE where $x(n)$ is a sinewave with reference frequency $\omega_0 = \pi/4$ and $\mu = 0.005$. These four different operating modes describe the capability of the ANE to reshape the residual noise. For $\beta = 0$, ANE behaves like a perfect notch filter to cancel the noise completely. For $\beta = 0.5$, the system attenuates 6 dB of the noise. At $\beta = 1$, the system allows all noise to pass. For $\beta = 2$, the system amplifies the noise with a gain equal to 2.

3. Passband disturbance reduction

The narrowband ANC assumes that the primary noise and internally generated sinusoidal reference signal have the same number of narrowband components with the same frequencies. If the primary noise contains other uncorrelated noise components, the ANC system will suffer from a passband disturbance due to the modulation effects of the secondary path. A technique developed in Ref. [10] for ANC systems will be modified to remove the uncorrelated noise components for ASQC systems.

We assume that the primary noise consists of sinusoidal components $u(n)$ and uncorrelated components $v(n)$ such that $d(n) = u(n) + v(n)$. By defining the weight error vector in steady state as $\mathbf{f}(n) = \mathbf{w}(n) - \mathbf{w}^o$ where $\mathbf{w}^o$ is

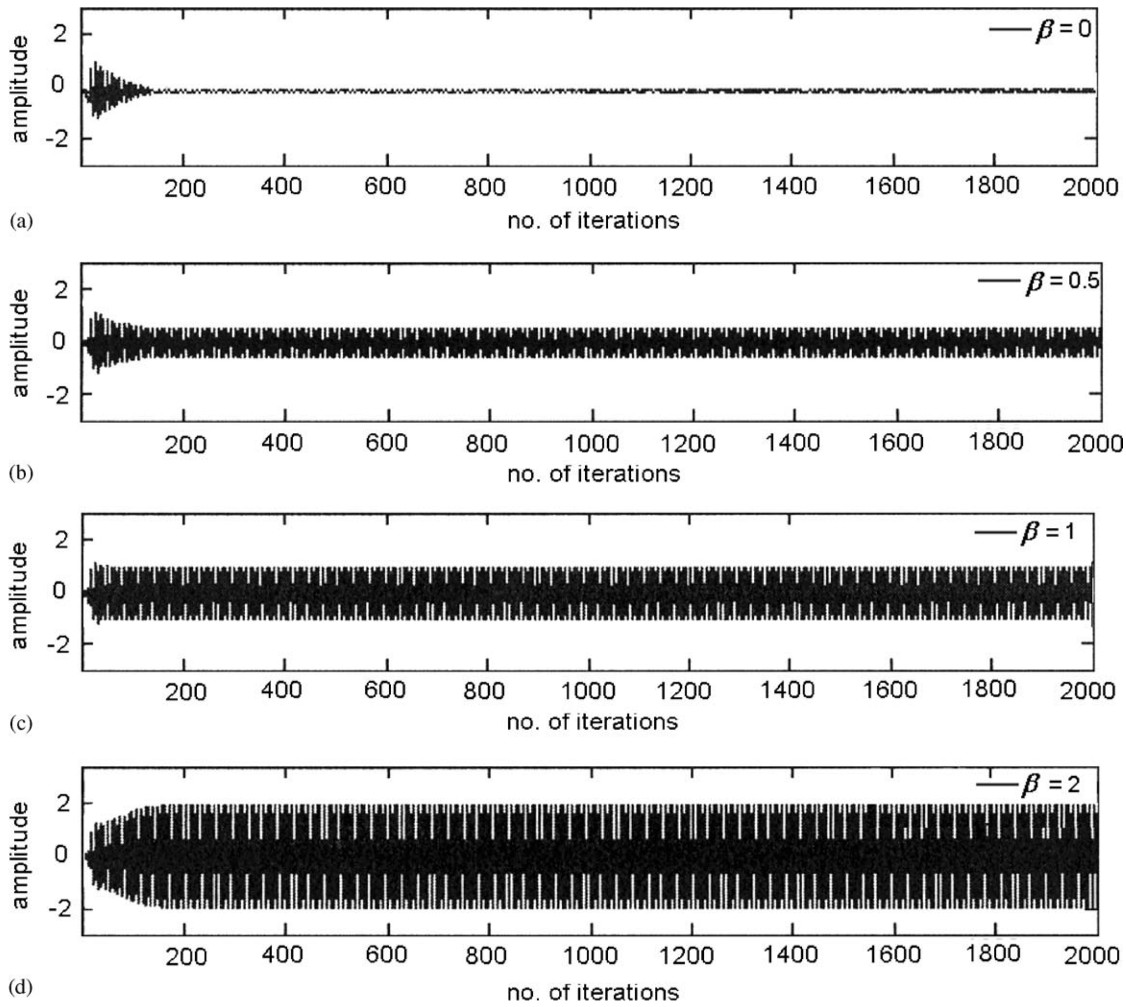

Fig. 3. Waveforms of residual noise at (a) $\beta = 0$, (b) $\beta = 0.5$, (c) $\beta = 1$, (d) $\beta = 2$.

the optimum solution, it is shown [10] that

$$\mathbf{f}(n+1) = \mathbf{f}(n) + 2\mu[u(n) - y'(n)][s(n)^{*}\mathbf{x}(n)] + 2\mu v(n)[s(n)^{*}\mathbf{x}(n)], \tag{8}$$

where $s(n)$ is the impulse response of $S(z)$, and * denotes linear convolution. The last term, $2\mu v(n)[s(n)^{*}\mathbf{x}(n)]$, is the perturbation that causes the passband disturbance. This undesired interference is proportional to the uncorrelated noise $v(n)$ and step size μ, and is related to the secondary path $S(z)$. One way to control this interference is by reducing the step size, but this would slow down the convergence. An effective way to control this effect is to introduce another adaptive filter to attenuate the interference in the measured residual noise $e(n)$ [10].

Including the secondary path, the transfer function of ANE with the FXLMS algorithm given in Eq. (4) becomes

$$H(z) = \frac{z^2 - 2z\cos(\omega_0) + 1 + 2\mu\beta AC^2 S(z)[z\cos(\omega_0 - \psi) - \cos(\psi)]}{z^2 - 2z\cos(\omega_0) + 1 + 2\mu AC^2 S(z)[z\cos(\omega_0 - \psi) - \cos(\psi)]}, \tag{9}$$

where C is the amplitude of the reference signal, ϕ the initial phase, ψ the phase shift of $S(\omega_0)$ and A the gain of $S(\omega_0)$. It is evident that the characteristics of $H(z)$ are affected by both the amplitude and phase responses of secondary path $S(z)$.

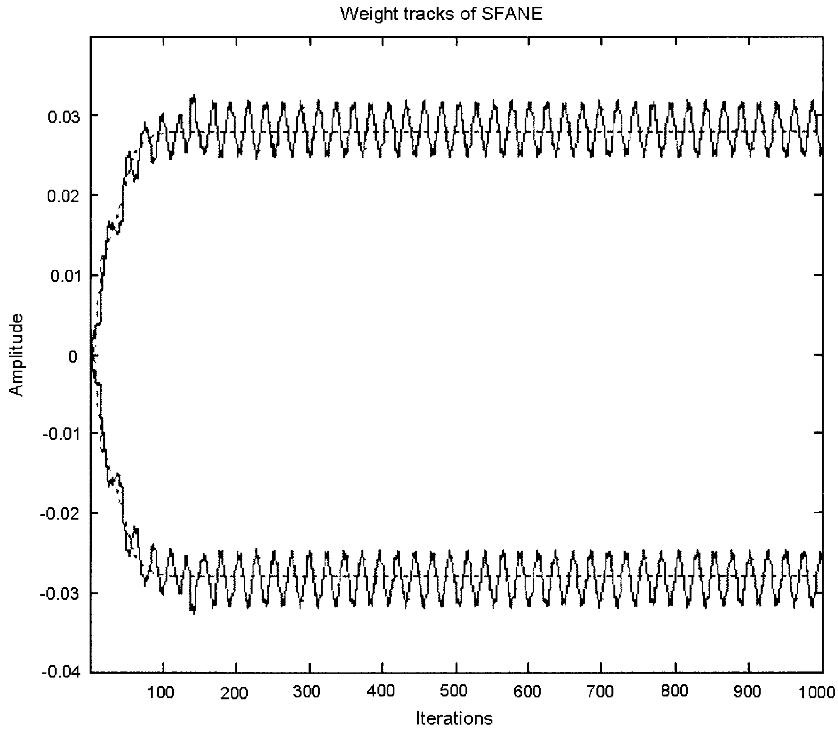

Fig. 4. Weight tracks of ANE with and without uncorrelated noise components, - - - - without uncorrelated noise, ——— with uncorrelated noise.

Computer simulations illustrate weight tracks due to the uncorrelated noise components. The dotted line in Fig. 4 shows the tracking of the ANE system for $\mu = 0.005$, and $x(n) = \cos(0.2\pi n)$ without interference, i.e., $u(n) = d(n) = \cos(0.2\pi n)$; while the solid line shows the results for $d(n) = \cos(0.2\pi n) + \cos(0.283\pi n)$. The simulation results clearly show that the uncontrolled noise $v(n)$ (the sinewave of frequency 0.283π) causes the weights to oscillate even after they reach the optimum solution (the flat dotted line).

The filtered-error LMS (FELMS) [10] approach employs an extra adaptive filter $C(z)$ (shown in Fig. 5) to remove the uncorrelated noise components from $e(n)$, thus reducing the undesired passband amplification. This second adaptive filter $C(z)$ also uses the LMS algorithm to minimize the instantaneous squared error signal $e_c(n)$, and is expressed as

$$\mathbf{c}(n+1) = \mathbf{c}(n) + \mu_c e_c(n)\,\mathbf{x}(n), \tag{10}$$

where μ_c is the step size. This algorithm can reduce the weight vector perturbation shown in Fig. 4 in the presence of a passband disturbance.

The basic principle of this FELMS algorithm is to purify $e(n)$. The adaptive filter $C(z)$ used in this algorithm acts like a bandpass filter with the center frequency as the reference frequency, thus rejecting interference at other frequencies. Therefore, the filtered $e(n)$ reduces the effects of uncorrelated noise on the adaptive filter. In the case where the noise frequency is changing slowly, the FELMS algorithm can use a large step size, thereby also increasing the convergence rate. The transfer function of the adaptive comb filter $H_c(z)$ can be written as [10]

$$H_c(z) = \frac{2\mu_c C^2[z\cos(\omega_0) - 1]}{z^2 - 2z(1-\mu_c C^2)\cos(\omega_0) + (1 - 2\mu_c C^2)}. \tag{11}$$

This equation is similar to a second-order infinite-impulse response filter, with complex conjugate poles on the unit circle. The pole radius $r = (1 - 2\mu_c C^2)^{1/2}$ determines the bandwidth of the filter, and a radius r closer to 1 results in narrower bandwidth. Thus, $H_c(z)$ acts like a bandpass filter with the

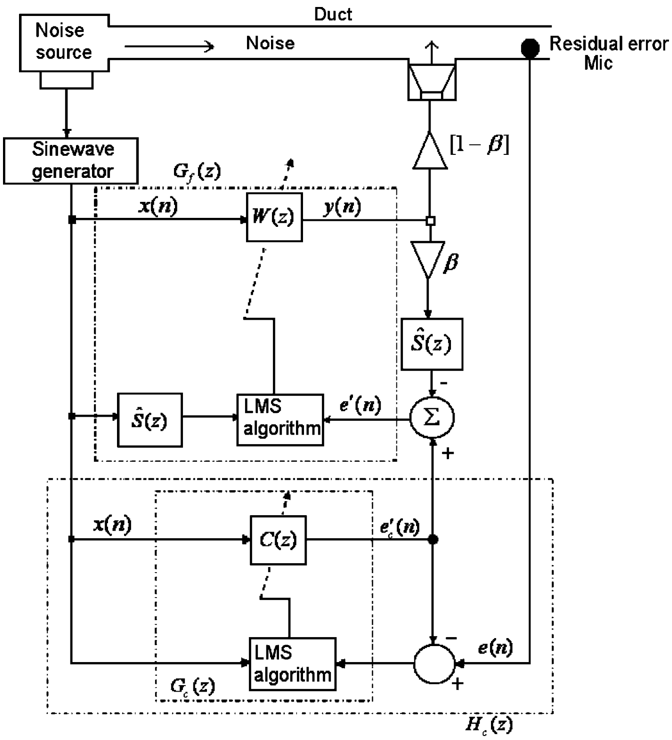

Fig. 5. Block diagram of ANE system with the FELMS algorithm.

peak frequency at

$$\gamma = \frac{(1 - \mu_c C^2)\cos(\omega_0)}{\sqrt{1 - 2\mu_c C^2}}. \tag{12}$$

Eq. (12) shows that when μ_c is very small, the frequency of the peak response is close to the reference frequency ω_0, i.e., $\gamma \cong \omega_0$. At that peak frequency, the transfer function $H_c(z)$ becomes

$$H_c(z)\big|_{z=r\exp(j\gamma)} \approx 1, \tag{13}$$

where $r \approx 1$. This property guarantees that the pseudo error $e'(n)$ with frequency γ will remain unchanged in the presence of a noise component in the residual noise $e(n)$. Hence, the introduction of $H_c(z)$ does not change the characteristics of ASQC systems.

Computer simulations in Fig. 6 compare the performance of the ANE system with the FXLMS and FELMS algorithms. The input signal is a unity amplitude sinewave at the reference frequency $\omega_0 = 0.125\pi$ and the uncorrelated noise is also a sinewave at frequency $\omega_1 = 0.283\pi$. Step sizes $\mu = 0.005$ and $\mu_c = 0.01$ are used for the simulations. It is evident that by employing the FELMS algorithm, the uncorrelated noise at $\omega_1 = 0.283\pi$ in the output is attenuated.

4. Convergence improvement

The FELMS algorithm introduced in the previous section effectively reduces a passband disturbance for ASQC systems. However, the system will still converge slowly at frequencies corresponding to the valleys of the magnitude response of the secondary path $S(z)$. To compensate for this effect, the FELMS algorithm is optimized such that the reference signal is a combination of sinusoids with normalized amplitudes according to the magnitude response of the secondary path.

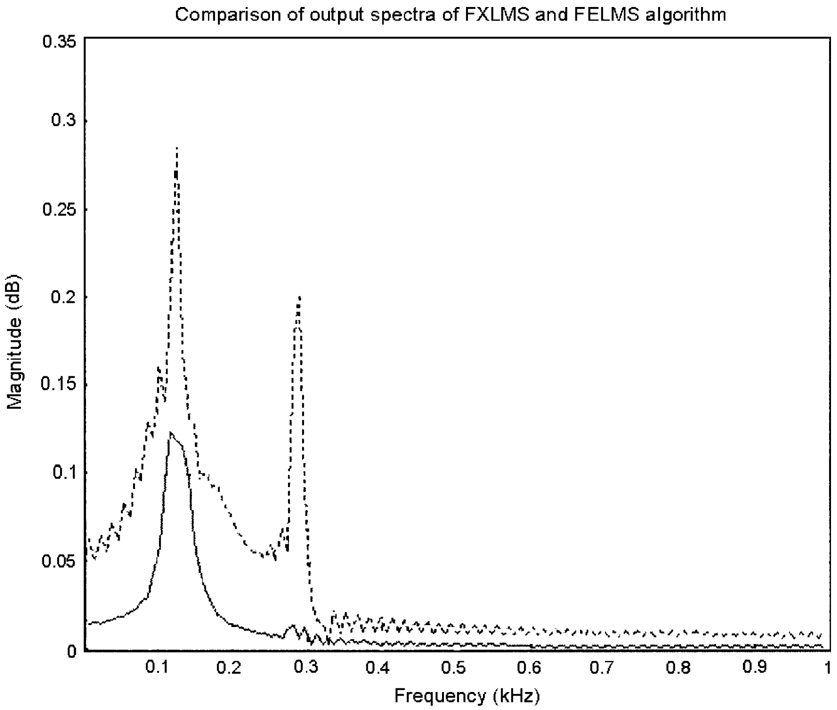

Fig. 6. Comparison of amplitude responses of ASQC system with the FXLMS and FELMS algorithms, – – – – FXLMS algorithm, ——— FELMS algorithm.

The convergence speed of the LMS algorithm is determined by the eigenvalue spread of the input autocorrelation matrix **R**. The eigenvalue spread of the system shown in Fig. 5 is [11]

$$\frac{\lambda_{\max}}{\lambda_{2K}} \geqslant \frac{\max_{k=1}^{K} A_k^2 S_k^2}{2 \min_{k=1}^{K} A_k^2 S_k^2}, \tag{14}$$

where $S_k = |S(\omega_k)|$ is the gain of $S(z)$ at frequency ω_k, $A_k = 1$, and λ_{2K} is the smallest nonzero eigenvalues of the matrix **R**. Here, λ_{2K} is used since the smallest nonzero eigenvalue is the 2Kth eigenvalue of **R** if the eigenvalues are arranged in descending order. Eq. (14) indicates that if the magnitude response of the secondary path is not flat, the algorithm converges slowly. If the amplitude of the sinusoid at frequency ω_k is normalized as

$$A_k = \frac{1}{S_k} \cong \frac{1}{|\hat{S}(\omega_k)|}, \quad k = 1, 2, \ldots, K \tag{15}$$

such that $A_k S_k = 1$, then Eq. (14) becomes a constant $\frac{1}{2}$. Thus, the amplitudes of sinusoids are inversely proportional to the magnitude response of the secondary path at the corresponding frequencies, and therefore, the system would converge faster than the conventional system.

Computer simulations are conducted to verify the performance of the optimized algorithm, in which the primary noise consists of eight harmonic related sinusoids with fundamental frequency $\omega_0 = 0.0625\pi$, and harmonics $\omega_1 = 0.125\pi$, $\omega_2 = 0.1875\pi$, $\omega_3 = 0.25\pi$, $\omega_4 = 0.3125\pi$, $\omega_5 = 0.375\pi$, $\omega_6 = 0.4375\pi$, $\omega_7 = 0.5\pi$. The step sizes used for the simulations were $\mu = 0.000005$ for $W(z)$ and $\mu_c = 0.0005$ for $C(z)$. In the optimized FELMS algorithm, the reference signal is a combination of the same eight harmonically related sinusoids with amplitudes according to Eq. (15). The learning curves of both the conventional and optimized FELMS algorithms are shown in Fig. 7. Here, the error signal of the optimized algorithm reaches zero within 600 iterations, whereas the traditional algorithm takes much longer. Hence, the ASQC system using the

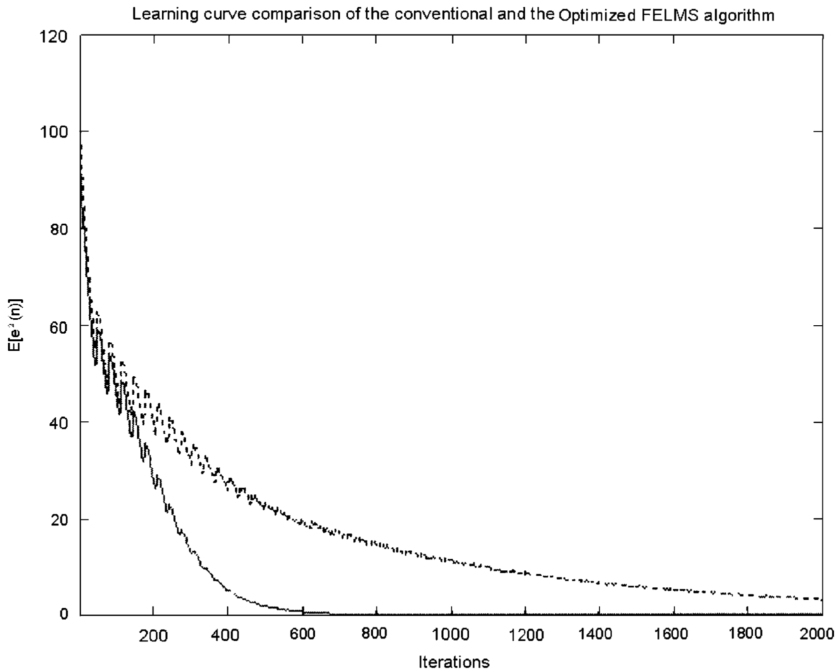

Fig. 7. Learning curves of ASQC system with FELMS algorithms, - - - conventional FELMS algorithm, —— optimized FELMS algorithm.

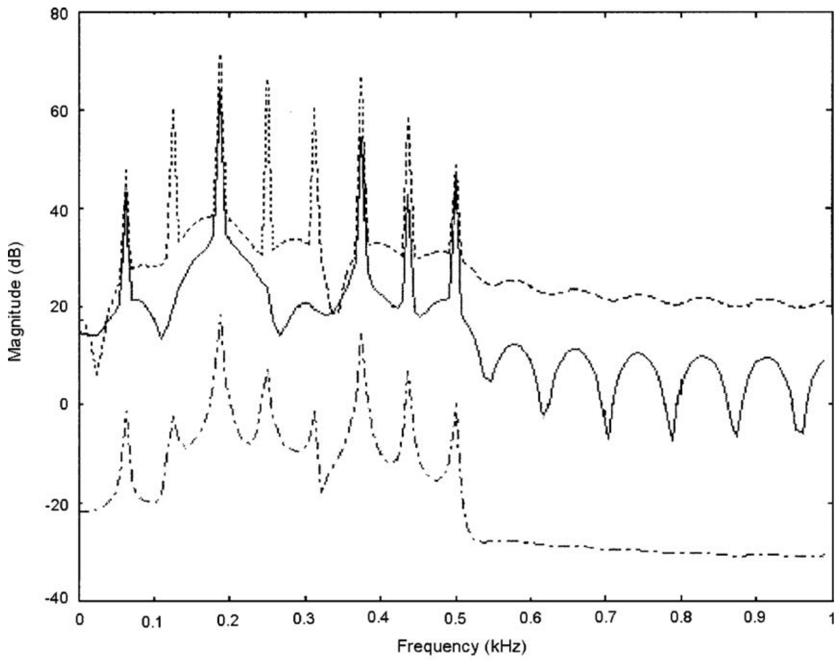

Fig. 8. Spectral comparison of ASQC system with conventional and optimized FELMS algorithms, – – – – primary noise, ——— conventional FELMS, – – – – optimized FELMS.

normalized FELMS algorithm converges faster than the traditional FELMS algorithm. This is evident from Fig. 8 where the convergence of the system using the conventional algorithm is affected significantly at the normalized frequencies 0.19, 0.375, and 0.5. These frequencies are the valley frequencies of the magnitude response of $S(z)$. The optimized FELMS algorithm reduces the noise components at those valley frequencies as predicted theoretically.

5. Conclusions

The ASQC system based on the ANE system with the optimized FELMS algorithm has been developed, tested, and analyzed. Simulations show that this new system can shape the residual noise spectrum, thus effectively controlling the sound quality or signature. This new system also reduces passband disturbance, which is caused by uncorrelated noise components in the primary noise that are amplified by the secondary path. Faster convergence can be achieved by using reference sinusoids with normalized amplitudes instead of unity amplitude. Therefore, the ASQC system developed in this paper provides faster convergence with reduced passband disturbance while controlling the sound quality.

References

[1] S.M. Kuo, D.R. Morgan, *Active Noise Control Systems—Algorithms and DSP Implementations*, Wiley, New York, 1996.
[2] S.M. Kuo, D.R. Morgan, Active noise control: a tutorial review, *Proceedings of the IEEE* 8 (1999) 943–973.
[3] G.W.B. Chaplin, The cancellation of repetitive noise and vibration, *Proceedings of the Inter-Noise* (1980) 699–702.
[4] S.J. Elliott, P. Darlington, Adaptive cancellation of periodic, synchronously sampled interference, *IEEE Transactions on Acoustics, Speech and Signal Processing* ASSP-33 (1985) 715–717.
[5] D.R. Morgan, An analysis of multiple correlation cancellation loops with a filter in the auxiliary path, *IEEE Transactions on Acoustics, Speech and Signal Processing* ASSP-28 (1980) 454–467.
[6] S.M. Kuo, M.J. Ji, Development and analysis of an adaptive noise equalizer, *IEEE Transactions on Speech and Audio Processing* 3 (1995) 217–222.
[7] S.M. Kuo, M.J. Ji, Principle and application of adaptive noise equalizer, *IEEE Transactions on Circuits and Systems II* 41 (1994) 471–474.
[8] S.M. Kuo, M. Tahernezhadi, L. Ji, Frequency-domain periodic active noise control and equalization, *IEEE Transactions on Speech and Audio Processing* 5 (1997) 348–358.
[9] S.M. Kuo, Y. Yang, Broadband adaptive noise equalizer, *IEEE Signal Processing Letters* 3 (1996) 234–235.
[10] S.M. Kuo, M.J. Ji, Passband disturbance reduction in adaptive narrowband noise control system, *IEEE Transactions on Speech and Audio Processing* 4 (1996) 96–103.
[11] S.M. Kuo, M. Tahernezhadi, W. Hao, Convergence analysis of narrowband active noise control systems, *IEEE Transactions on Circuits System I* 46 (1999) 220–223.
[12] S. Mallu, Integration and Optimization of Active Noise Equalizer with Filtered Error Least Mean Square Algorithm, MS Thesis, Northern Illinois University, 2005.
[13] B. Widrow, S.D. Stearns, *Adaptive Signal Processing*, Prentice-Hall, Englewood Cliffs, NJ, 1985.